Available online at www.sciencedirect.com

SciVerse ScienceDirect

Energy Procedia 12 (2011) 966 – 974

Energy Procedia

ICSGCE 2011: 27–30 September 2011, Chengdu, China

Comparison of Sliding Mode and PI Control of a Hybrid Energy Storage System in a Microgrid Application

A. Etxeberria[a,b*], I. Vechiu[a], H. Camblong[a,c], J.-M. Vinassa[b]

[a] *ESTIA-Recherche, the Research Division of Ecole Supérieure des Technologies Industrielles Avancées (ESTIA), Technopôle Izarbel, 64210 Bidart, France*

[b] *Laboratoire IMS CNRS UMR 5218, Université Bourdeaux 1, 33405 Talence Cedex, France*

[c] *University of Basque Country, Europa plaza 1 (E.U.P-D), 20018 Donostia-San Sebastian, Spain*

Abstract

A high penetration of the Renewable Energy Sources (RES) can create stability, reliability and power quality problems in the main electrical grid due to their stochastic nature. The microgrid is one of the analysed solutions to solve this problem. In this context, the storage becomes necessary to better harness the energy generated by RES and to maintain the proper operation of the microgrid.

This paper addresses the control of the bidirectional DC-DC converters used to interface a parallel connected Hybrid Energy Storage System (HESS) formed by a Vanadium Redox Battery (VRB) and a SuperCapacitor (SC) bank. The linear controllers have been widely used due to their simple design and implementation. However, their operation is limited to a certain operation range. The variability of the analysed system makes the use of a more robust controller necessary. In this work a PI based two-loop control system and a PI type sliding mode controller (SMC) are compared by means of simulations using the Matlab-Simulink software. Some rules are fixed to facilitate the design process of the SMC and the advantages of using a nonlinear controller are stressed.

Selection and/or peer-review under responsibility of University of Electronic Science and Technology of China (UESTC)

Keywords: batteries; DC-DC power converters; energy storage; renewable energy; sliding mode control; supercapacitors.

1. Introduction

The microgrid is one of the systems that is being analysed as a solution to the integration of the Renewable Energy Sources (RES). Generally, a microgrid can be defined as a weak electrical grid formed by different microsources (both renewable and not renewable sources), energy storage devices, power conversion systems and different controllers. The main characteristic of a microgrid is its ability to work

* Corresponding author. Tel.: +33 5 59 43 85 06

E-mail address: a.etxeberria@estia.fr

doi:10.1016/j.egypro.2011.10.127

connected to the main grid or in islanding mode [1].

The use of an energy storage system (ESS) is necessary in order to smooth the variability of the RES and other variations that can occur in a microgrid. An ESS must have a high power density in order to face fast power variations, and at the same time a high energy density, to give autonomy to the microgrid. As nowadays there is not any storage technology that satisfies both requirements, it is necessary to associate more than one storage device creating a Hybrid Energy Storage System (HESS) [2].

In this work a HESS based on the association of a Vanadium Redox Battery (VRB) as long-term storage device and a SuperCapacitor (SC) bank as short-term storage device is investigated in order to improve the microgrid operation during RES and load variations. The parallel topology has been selected to interface each storage device with the DC bus, using bidirectional DC-DC converters (BDC) to connect each device.

This paper focuses on the control part of the BDCs. The linear controllers have been used in different works to control storage systems though bidirectional converters [3], [4]. However, these controllers are designed to manage the system around an operating point and they cannot assure a good response with high load variations or parameter uncertainty. Nonlinear controllers, on the other hand, are more robust controllers that can face those kinds of variations.

This work compares by means of simulations the response of a PI type sliding mode control (SMC) system and a typical two-loop PI based control system. The simulations have been carried out using the Matlab/Simulink software and the SimPowerSystems toolbox.

2. Hybrid Energy Storage System Modeling

This section shows the dynamic models of the two ESSs that have been used during simulations. The complexity of the dynamic models has been chosen according with the investigated phenomena.

2.1. Supercapacitor

The SC is represented using a series connected RC circuit formed by a constant capacitor and a constant resistance, which represents the electronic serial resistance in the conductors and the ionic resistance in the electrolyte. From different literature works [5] it is clear that both capacitance and the serial resistance of the SC are dependent on frequency, temperature and voltage. However, in the simulations that have been run, the simulation time is short and thus the effect of the temperature and voltage variations can be neglected because they are almost constant. The self-discharge has been neglected due to the same reason. The frequency variations of the supercapacitor current are low enough to assume that the capacitor value is also constant.

2.2. Vanadium redox battery

The dynamic model used to represent the VRB has been presented in detail in [6]. The model was presented in those works as a valid dynamic model to simulate the effect of a VRB for wind power smoothing application. The stack voltage is modelled as a controlled voltage source, being its value dependant on the state-of-charge (SOC) and the open circuit voltage or Nernst voltage. The SOC is modelled as a variable that is updated every simulation step. The transient behaviour of the VRB is represented using a parallel capacitance. This transient behaviour is related to the electrode capacitance as well as the concentration depletion close to the electrodes. In the used dynamic model only the electrode capacitance is represented.

The work [6] determine the parameters of the model assuming that at the operation point where the

stack current is maximum and the SOC 20%, the power losses of the VRB are of 21%. Therefore, at this operation point the overall efficiency is supposed to be 79%.

2.3. Bidirectional DC-DC converter

The well-known averaging method [7] has been used to represent the behaviour of the BDC (Fig. 1 shows the topology of the selected bidirectional converter). As the BDC can work in both senses, it is necessary to distinguish two averaged equation systems, the first related with the boost mode and the second related with the buck mode (1) and (2) with $a=1$ and $a=-1$ respectively).

$$\frac{dV_{bus}}{dt} = a\left(-\frac{i_{o1}}{C} + \frac{ui_L}{C}\right) \quad (1)$$

$$\frac{di_L}{dt} = a\left(\frac{V_{ess}}{L} - \frac{uV_{bus}}{L}\right) \quad (2)$$

3. Control of the HESS

Fig. 1 shows the schematic representation of the system that has been simulated. It is formed by a current source that emulates the current generated by a wind turbine, two BDCs that are used to interface the storage devices, a DC bus capacitor, a two-level inverter, a line and a resistive load. The inverter is controlled by a typical two-level PI based dq0 frame control system [8].

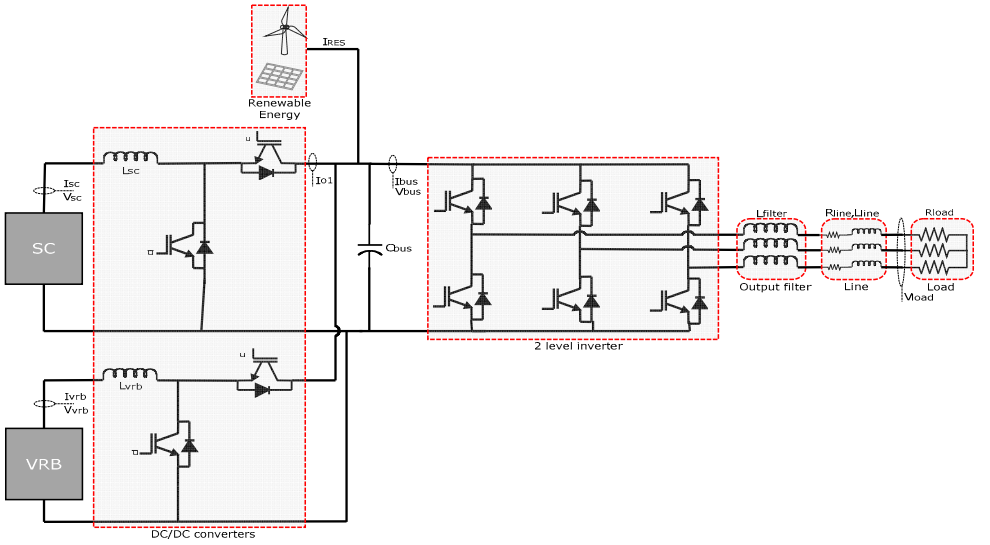

Fig. 1.Schematic representation of the analysed system.

In the case of the HESS there are two control levels, as shown in Fig. 2. The higher control level is responsible of selecting the power reference for each storage device. The low control algorithms control the power converters to follow the power references. There are many different control methods for the high level control system [6], [9]. In this case the filtering one has been selected. The power absorbed by the inverter is filtered and the low-frequency part is supplied by the VRB. The DC bus voltage control is made by the SC, using a two-loop control strategy. Thus, the SC tends to supply/absorb a constant

current. Consequently, the power supplied/absorbed by the SC is also filtered and the low frequency part is added to the VRB current reference in order to maintain at 0A the average current of the SC.

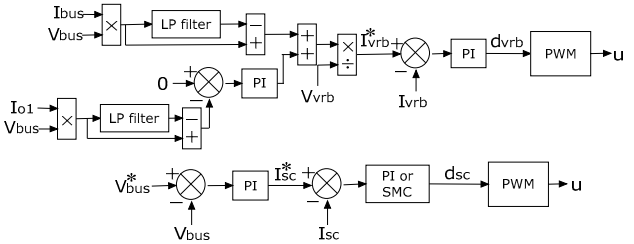

Fig. 2: Structure of the control system.

The low-level control algorithm of a BDC is typically a two-loop PI control system. The proper operation of the linear controllers is limited to an operation range around the selected operation point, and in consequence it is not possible to assure that it will be able to face the different variations that can occur in the system. In the case of the HESS application in the microgrid context, system variables like the voltage of the storage devices can have high variations. A more robust control algorithm may be necessary to control the system in order to face these variations as well as the inevitable parameter uncertainty made in the modelling process of the system.

This work proposes a sliding mode control system to control the BDC of the SC, as it is the one that will face fast power variations. The low-level current control of the VRB is carried out by a PI. The behaviour of the SMC is compared with the response of a PI based control system, showing some results that justify the use of a nonlinear controller from the control point of view.

The typical hysteresis-modulation based sliding mode controllers create a variable switching frequency, which complicates the design of the output filters and increase the power losses of the BDCs. From the power conversion system's point of view a fixed-frequency should be used. In this work a PWM based modulation has been used to fix the switching frequency of the SMC.

The following two subsections explain the design process of the SMC and PI control systems of the BDC.

3.1. PI control system design

This control system is based on the use of two control loops, an inner one to control the current of the inductance and the outer one to control the DC bus voltage, as it is shown in the Fig. 2. A PI is used for each loop.

In this case, the boost mode equations are going to be used to design the controller. Same controllers but with opposite sign parameters could be obtained using the buck mode equations.

The system represented by(1)and (2) is not linear. Thus, it is not linear. Thus, it is not linear. Thus, it is necessary to linearise the equations in order to obtain the different transfer functions and be able to design the controller [10]. Neglecting the effect of the small variations of the other inputs, the small-signal transfer function (1) has been obtained, which can be used to design the inner current loop.

$$\frac{\tilde{i}_L}{\tilde{d}} = \frac{-CV_{BUS}s - DI_L}{CLs^2 + D^2} \qquad (3)$$

A PI controller has been designed using the Matlab rltool() function. Its values K_{pI} and T_{iI} are shown in

Table 1. The current PI controller of the BDC of the VRB has been designed by this method.

Once the inner control loop has been designed, it is necessary to take into account its effect in order to design the outer control loop of the DC bus voltage. The control action u is generated by a PI controller, whose expression is shown in (2). If this expression is substituted in the linearised equations, the new equation system will represent the behaviour of the inner closed loop system. Then, the transfer function (3) can be calculated and used to design the outer voltage control loop. The parameters of the PI voltage controller K_{p2} and T_{i2} are shown in Table 1.

Table 1: Control system parameters.

Parameter	Value	Parameter	Value
K_{p1}	-0.5	K_1	14.62
T_{i1}	-0.001	K_2	7311
K_{p2}	10	K_3	1
T_{i2}	0.0001		

$$\tilde{u} = \frac{\left(\tilde{i}_{Lref} - \tilde{i}_L\right)\left(K_{p1}T_{i1}s + 1\right)}{T_{i1}s} \tag{4}$$

$$\frac{\tilde{V}_{bus}}{\tilde{i}_{Lref}} = \frac{-K_{p1}T_{i1}DV_{BUS}s - DV_{BUS}}{CLTs^3 - CV_{BUS}K_{p1}T_{i1}s^2 + \left(D^2T_{i1} - CV_{BUS}\right)s} \tag{5}$$

3.2. SMC design

A nonlinear controller has been designed in order to analyse its advantages comparing to the linear controller. The sliding mode control has been selected due to its ability to guarantee stability and robustness against parameter, line and load uncertainties [11]. As the power converters are inherently variable structure systems, the use of the SMC is appropriate to control such kind of systems.

The selected switching surface is shown in (4), whose structure can be named as PI type SMC (refer to Fig. 2). The effect of the inductor current, third element of the surface, is added in the case of the buck mode and subtracted in the boost mode, as the positive current sense has been selected as the one that discharges the ESS.

The steps to design a SMC controller for a DC-DC converter can be found in [11]. The hitting condition is met with the configuration shown in (4).

$$S = K_1X_1 + K_2\int X_1dt \pm K_3X_2$$

$$u = \begin{cases} 1, & when\ S < 0 \\ 0, & when\ S > 1 \end{cases} \tag{6}$$

where $X_1 = V_{busref} - V_{bus}$ and $X_1 = i_L$

Once the hitting condition is satisfied, it is necessary to analyse the existence condition of the SMC controller applying the local reachability condition of the state trajectory (5):

$$\lim_{S\to 0} S\dot{S} < 0 \tag{7}$$

In order to analyse the existence condition, first of all it is necessary to transform the averaged equations of the BDC using the new state variables (refer to (6) and (7), boost mode with *a=1* and buck mode with *a=-1*).

$$\frac{dX_1}{dt} = a\left(\frac{i_{o1}}{C} - \frac{uX_2}{C}\right) \tag{8}$$

$$\frac{dX_2}{dt} = a\left(\frac{V_{ess}}{L} + \frac{uX_1}{L} - \frac{uV_{busref}}{L}\right) \tag{9}$$

The existence condition is analysed dividing the problem in two cases.

Case 1: When S<0, $\dot{S}$ >0 and u=1

$$\dot{S} = K_1 a\left(\frac{i_{o1}}{C} - \frac{uX_2}{C}\right) + K_2 X_1 \pm K_3 a\left(\frac{V_{ess}}{L} + \frac{uX_1}{L} - \frac{uV_{busref}}{L}\right) > 0 \tag{10}$$

Case 2: When S>0, $\dot{S}$ <0 and u=0

$$\dot{S} = K_1 a\frac{i_{o1}}{C} + K_2 X_1 \pm K_3 a\frac{V_{ess}}{L} < 0 \tag{11}$$

The selected sliding coefficients must assure that both inequalities, (8) and (9), are satisfied.

However, these inequalities are not helpful to analyse which can be the limits of the parameters. An interpretation of those expressions can conclude in new simplified relations that can be used to select the sliding coefficients.

In the inequality (8), if $u=0$ is substituted in the state equations, the transform of Laplace is applied and the final values of the state variables are obtained, it can be seen that their tendencies are $X_1 \rightarrow V_{busref}-V_{ess}$ and $X_2 \rightarrow i_{bus}$. Knowing that, the inequality is satisfied for both operation modes if $K_2>0$.

In the inequality (9), if it is assumed that the DC bus voltage is near the reference value, the element K_2X_1 could be taken as negligible taking into account that the values of C and L are small enough to increase the other two addends in consideration. In that case, in the buck mode the inequality will be satisfied selecting positive values for K_1 and K_3; in the case of the boost mode, the relation (10) is obtained. Fixing the maximum current injected by the BDC in the DC bus, an upper limit for the relation between K_1 and K_3 can be defined.

$$\frac{K_1}{K_3} < \frac{V_{ess}C}{i_{o1}L} \tag{12}$$

After analysing the existence condition, the stability condition must be assured, which will give more limited rules to define the sliding coefficients. The stability condition of the SMC is guaranteed if the dynamic of the system in sliding mode is directed toward an operation point where a stable equilibrium exists [11]. In sliding mode the system slides in the switching surface and in consequence S <0 and $\dot{S}$ <0. The dynamic of the BDC in sliding mode can be obtained calculating the equivalent control from the expression $\dot{S}$ <0 (11) and substituting it in the average state equations ((6) and (7)). In this case only the equivalent control of the boost mode is used; the same transfer functions but with opposite sign can be obtained for the buck mode.

$$u_{eq} = \frac{K_1 i_{o1} L + K_2 X_1 CL - K_3 V_{ess} C}{K_1 X_2 L + K_3 C X_1 - K_3 C V_{busref}} \tag{13}$$

Once the equivalent control is substituted in the averaged equations, they must be linearised around an operating point as the obtained equations are highly nonlinear. Then, it is possible to obtain the small-signal transfer function between the output DC bus voltage error and the input DC bus current, which is a disturbance from the DC bus voltage point of view. If it is assumed that in the operating point the voltage error, the inductance current and the DC bus current are null, the expression of the transfer function is considerably simplified. Furthermore, if a value of *1* is selected for the parameter K_2, the second order

behaviour of the DC bus voltage can be represented depending on the values of K_1 and K_2. The resulting transfer function is shown in (12), and it represents the dynamic of the system in the sliding mode around the selected operating point. The relation between these parameters and the natural frequency and the damping factor can be obtained easily and the controller can be defined to obtain the desired dynamic.

The numerical values for K_1 and K_2 (refer to Table 1) have been selected in order to have a damping factor of $\xi=1$ and a settling time of *3 ms*.

$$\frac{\tilde{x}_1}{\tilde{i}_{bus}} = \frac{1}{C}\frac{1}{s^2 + \frac{V_{ESS}K_1}{CV_{BUS}}s + \frac{V_{ESS}K_2}{CV_{BUS}}} \quad (14)$$

4. Simulation Results

The investigated control algorithms have been compared in two different case studies that simulate two situations that occur in a microgrid. On the one hand, the effect of the variability of the RES has been simulated introducing a current profile generated by a wind turbine in the DC bus. On the other hand, the effect of an instantaneous AC load power increase has been simulated.

The parameters of the supercapacitor bank used in the simulations have been extrapolated from the commercial unit BMOD0083 P048 of Maxwell Technologies manufacturer. The parameters that have been used are equivalent of a SC bank that has 200 cells connected in series. The total capacity of the used SC is 3.75F, the serial resistance is 114.4mΩ and the maximum voltage is 540V.

The VRB used in this work has a rated stack voltage of 450V (at 50% of SOC and open circuit), a maximum charge/discharge current of 28A and an autonomy of 0.75 hours. The parameters used in this work are resumed on the left two columns of Table 2.

Table 2: Simulation parameters.

Parameter	Value	Parameter	Value
N	322	$f_{switching}$	15kHz
$V_{equilibrium}$	1.4V	L_{SC}	2mH
k	0.05138	L_{VRB}	2mH
K_{pump}	0.9877	C_{bus}	4700μF
$R_{resistive}$	0.972Ω	L_{filter}	3mH
$R_{reaction}$	1.458Ω	R_{line}	12mΩ
R_{fixed}	531.44Ω	L_{line}	211μH
$C_{electrodes}$	0.0186F	R_{load}	12Ω

The configuration of the simulation system has been shown in Fig. 1 and the other simulation parameters are given in Table 1 and Table 2.

Fig. 3 shows the results of the two case studies. When the current profile generated by a wind turbine is introduced to the DC bus, the behaviour of both control systems is similar, and thus, only the response of one of them is shown in Fig. 3a. The response of the controller is analysed in two cases, when the voltage of the SC is the rated one (450V) and the case when the SC is discharged with a voltage of 250V. As the variations introduced by the current profile are not very high and fast, both controllers react in a similar manner and both are able to maintain the stability of the system as well as to integrate correctly the energy coming from the wind turbine. Due to the filtering method, the SC supplies/absorbs the fast power variations coming from the RES, and the battery supplies the current that is necessary to maintain the average current of the SC at 0A (see Fig. 3a). The DC bus voltage is also maintained at the reference

700V value (see Fig. 3b).

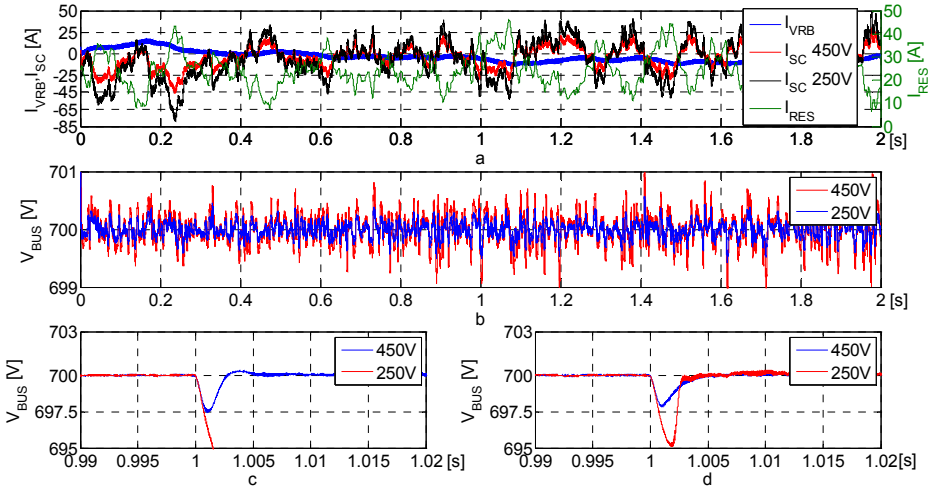

Fig. 3. a)RES variation-ESS current evolution, b)RES variation-DC bus voltage evolution, c)Load variation-DC bus voltage in PI case, d)Load variation-DC bus voltage in SMC case.

In the second case study an AC load power increase of 50% (13.5kW) is introduced. In Fig. 3c the response of the PI based controller is shown and in Fig. 3d the one of the SMC. In both cases only the DC bus voltage evolution is shown: the AC variables behaviour is correct and the inverter is able to restore the correct 230Vrms value after a short transient period. Due to the filtering method, the peak power is supplied entirely by the SC. As in the first case study, two responses are compared: first when the SC is at 450V and second when its voltage is 250V. The results show that the PI system is able to react as expected when the voltage of the SC is the one used to calculate the controller, but when the voltage is reduced the control system looses stability. On the other hand, the SMC is able to react maintaining the design specifications in both cases.

5. Conclusions

The control of a HESS in a microgrid application has been analysed, comparing a PI based linear controller and the nonlinear sliding mode control. The SMC controller design has been summarised, defining some rules that facilitate the selection of the sliding coefficients for the control of a bidirectional DC-DC converter.

The comparison between the responses of the controllers shows that the sliding mode control is able to react in a similar manner independently of the state-of-charge of the SC. However, the PI based control system is not able to maintain its good response when the operation point is not inside a limited range around the operating point selected to design the controllers. Due to the characteristics of the HESS and the microgrid operation, the PI based controller cannot assure the stability of the system in the entire operation range and consequently is not an acceptable option for this application. The sliding mode controller shows a higher robustness and it is able to operate correctly at the different cases that have been analysed.

Acknowledgment

The authors want to thank to Working Community of the Pyrenees for having supported this research work.

References

[1] B. Kroposki, R. Lasseter, T. Ise, S. Morozumi, S. Papatlianassiou, and N. Hatziargyriou, "Making microgrids work," IEEE Power and Energy Magazine, vol. 6, no. 3, pp. 40-53, Jun. 2008.

[2] P. J. Hall and E. J. Bain, "Energy-storage technologies and electricity generation," Energy Policy, vol. 36, no. 12, pp. 4352-4355, Dec. 2008.

[3] N. Mendis, K. M. Muttaqi, S. Sayeef, and S. Perera, "Application of a hybrid energy storage in a remote area power supply system," in Proc. IEEE EnergyCon, 2010, pp. 576-581.

[4] W. Li, G. Joos, and C. Abbey, "A Parallel Bidirectional DC/DC Converter Topology for Energy Storage Systems in Wind Applications," in Proc. IEEE 42nd IAS Annu. Meeting, 2007, pp. 179-185.

[5] W. Lajnef, J. M. Vinassa, O. Briat, S. Azzopardi, and E. Woirgard, "Characterization methods and modelling of ultracapacitors for use as peak power sources," J. Power Sources, vol. 168, no. 2, pp. 553-560, Jun. 2007.

[6] W. Li, G. Joos, and J. Belanger, "Real-Time Simulation of a Wind Turbine Generator Coupled With a Battery Supercapacitor Energy Storage System," IEEE Trans. Ind. Electron., vol. 57, no. 4, pp. 1137-1145, Apr. 2010.

[7] Junhong Zhang, Jih-Sheng Lai, and Wensong Yu, "Bidirectional DC-DC converter modeling and unified controller with digital implementation," in Applied Power Electronics Conference and Exposition, 2008. APEC 2008. Twenty-Third Annual IEEE, 2008, pp. 1747-1753.

[8] I. Vechiu, H. Camblong, G. Tapia, B. Dakyo, and O. Curea, "Control of four leg inverter for hybrid power system applications with unbalanced load," Energy Conversion and Management, vol. 48, no. 7, pp. 2119-2128, Jul. 2007.

[9] A. L. Allègre, R. Trigui, and A. Bouscayrol, "Different energy management strategies of Hybrid Energy Storage System (HESS) using batteries and supercapacitors for vehicular applications," in Vehicle Power and Propulsion Conference (VPPC), 2010 IEEE, 2010, pp. 1-6.

[10] L. Guo, J. Y. Hung, and R. M. Nelms, "Comparative evaluation of sliding mode fuzzy controller and PID controller for a boost converter," Electric Power Systems Research, vol. 81, no. 1, pp. 99-106, Jan. 2011.

[11] Siew-Chong Tan, Y. M. Lai, and C. K. Tse, "General Design Issues of Sliding-Mode Controllers in DC–DC Converters," IEEE Trans. Ind. Electron., vol. 55, no. 3, pp. 1160-1174, 2008.